F7030 Rentgenový rozptyl na tenkých vrstvách

O. Caha
PřF MU

Prezentace k přednášce
Numerické simulace
Příklady experimentů
Vybrané vztahy

Sylabus

1. Experimentální technika: zdroje, vznik rtg záření, goniometry, optické prvky (monochromátory, kolimátory, zrcadla, fokusační optika), detektory. Základní experimenty: polykrystalové a monokrystalové metody, mapování reciprokého prostoru

2. Kinematická teorie rozptylu: úvod do teorie rozptylu, rozptyl na elektronu, izolovaném atomu, krystal, strukturní a geometrický faktor, omezená velikost krystalu

3. Difrakce na polykrystalech I: strukturní faktor, velikost krystalitu (Scherrerova formule), vliv deformace na polohy a šířky difrakčních maxim, zbytková napětí, kvantifikace fázového složení (vnitřní normál)

4. Polykrystaly II: Full profile fitting; Textury, ODF (orientation distribution function); Debyeův vztah, PDF (pair distribution function).

5. SAXS: teoretický popis, řídké roztoky – Guinierův a Porodův vztah, uspořádané částice – long range a short-range order

6. Dokonalé, téměř dokonalé krystaly, epitaxní vrstvy: Kinematická teorie na monokrystalu a epitaxní vrstvě – polohy difrakcí, truncation rod, deformace v epitaxní vrstvě, relaxace. Mozaikový krystal

7. Dynamická teorie rtg reflexe: Jednovlnná aproximace – hloubka vniku, reflexe na hladkém rozhraní, multivrstvy (formalismus přenosové matice), TRXRF

8. Dynamická teorie rtg difrakce: Dvojvlnná aproximace: případ Bragg a Laue, Borrmannův jev, stojatá vlna, GID, epitaxní vrstvy

9. Semikinematická teorie I: DWBA, Rozptyl na drsných rozhraních – popis drsného rozhraní, příklady: fraktálové rozhraní, dvouúrovňové, vicinální, spekulární odraz a nespekulární rozptyl, drsné multivrstvy

10. Semikinamatická teorie II: GISAXS na částicích na povrchu a uvnitř vzorku, Difuzní rozptyl na defektech v krystalu v okolí difrakce

11. Experimentální rozlišení Experimentální rozlišení v reciprokém prostoru: analyzer streak, detector streak, monochromator streak, DuMondovy grafy, disperzní a nedisperzní uspořádání, koherenční šířka a délka

12. Další rentgenové metody: Fluorescenční spektroskopie, absorpční spektroskopie – XAFS, XMCD.

Kinematická teorie difrakce

$$\hat{\mathbf{T}} \approx \hat{\mathbf{V}}$$

$$E_s(\boldsymbol{r}) = \int \mathrm{d}^3\boldsymbol{r'} G_0(\boldsymbol{r} - \boldsymbol{r'}) \hat{\mathbf{V}}(\boldsymbol{r'}) E_i(\boldsymbol{r'})$$

$$E(\boldsymbol{r}) = 4\pi r_{\mathrm{el}} C E_i \int \mathrm{d}^3\boldsymbol{r'} G_0(\boldsymbol{r} - \boldsymbol{r'}) \varrho(\boldsymbol{r'}) \mathrm{e}^{\mathrm{i}\boldsymbol{K}_i.\boldsymbol{r'}}$$

turbance of the sample structure. A simple (but not always valid) qualitative rule says that the kinematical approximation can be used if at least one of the following conditions is met:

- the length of the trajectory of the x-rays in the sample is sufficiently small
- the layer is highly disturbed
- the angular deviation of the primary x-ray beam from the direction of the diffraction maximum is sufficiently large.

Kinematická teorie

$$\chi(\boldsymbol{r}) = -r_{\mathrm{el}}\frac{\lambda^2}{\pi}\varrho(\boldsymbol{r})$$

$$\chi(\boldsymbol{r}) = \sum_{\boldsymbol{g}} \chi_{\boldsymbol{g}} \mathrm{e}^{\mathrm{i}\boldsymbol{g}.\boldsymbol{r}}$$

$$\chi_{\boldsymbol{g}} = \frac{1}{V_{\mathrm{el}}} S_{\mathrm{el}}(\boldsymbol{g});\ S_{\mathrm{el}}(\boldsymbol{g}) = \int_{\mathrm{V_{el}}} \mathrm{d}^3\boldsymbol{r}\ \chi(\boldsymbol{r})\mathrm{e}^{-\mathrm{i}\boldsymbol{g}.\boldsymbol{r}}$$

$$S_{\mathrm{el}}(\boldsymbol{g}) = -\frac{4\pi r_{\mathrm{el}}}{K^2}\sum f_j(\boldsymbol{g})\mathrm{e}^{-\mathrm{i}\boldsymbol{g}.\boldsymbol{r}_j}$$

$$f(\boldsymbol{Q}) = \int \mathrm{d}^3\boldsymbol{r}\varrho(\boldsymbol{r})\mathrm{e}^{-\mathrm{i}\boldsymbol{Q}.\boldsymbol{r}} = \frac{4\pi}{Q}\int_0^\infty \mathrm{d}r\varrho(r)\sin(Qr)$$

Kinematická teorie

$$\mathbf{R_n} = n_1\,\mathbf{a}_1 + n_2\,\mathbf{a}_2 + n_3\,\mathbf{a}_3$$

$$F^{crystal}(\mathbf{Q}) = \sum_{\ell}^{\text{All atoms}} f_\ell(\mathbf{Q})\mathrm{e}^{i\mathbf{Q}\cdot\mathbf{r}_\ell}$$

$$F^{crystal}(\mathbf{Q}) = \sum_{\mathbf{R}_n+\mathbf{r}_j}^{\text{All atoms}} f_j(\mathbf{Q})\mathrm{e}^{i\mathbf{Q}\cdot(\mathbf{R}_n+\mathbf{r}_j)} = \overbrace{\sum_{\mathrm{n}} \mathrm{e}^{i\,\mathbf{Q}\cdot\mathbf{R_n}}}^{\text{Lattice}} \overbrace{\sum_{j} f_j(\mathbf{Q})\mathrm{e}^{i\,\mathbf{Q}\cdot\mathbf{r}_j}}^{\text{Unit cell}}$$

$$F^{u.c.}(\mathbf{Q}) = \sum_{j} f_j(\mathbf{Q})\mathrm{e}^{i\,\mathbf{Q}\cdot\mathbf{r}_j}$$

$$\mathbf{a}_i \cdot \mathbf{a}_j^* = 2\pi\,\delta_{ij}$$

$$\mathbf{G} = h\,\mathbf{a}_1^* + k\,\mathbf{a}_2^* + l\,\mathbf{a}_3^*$$

$$\mathbf{Q} = \mathbf{G}$$

$$\mathbf{G}\cdot\mathbf{R_n} = 2\pi(hn_1 + kn_2 + ln_3)$$

Kinematická teorie

$$\mathbf{a}_1^* = \frac{2\pi}{v_c}\,\mathbf{a}_2 \times \mathbf{a}_3 \qquad \mathbf{a}_2^* = \frac{2\pi}{v_c}\,\mathbf{a}_3 \times \mathbf{a}_1 \qquad \mathbf{a}_3^* = \frac{2\pi}{v_c}\,\mathbf{a}_1 \times \mathbf{a}_2 \qquad v_c = \mathbf{a}_1 \cdot (\mathbf{a}_2 \times \mathbf{a}_3)$$

$$S_N(\mathrm{Q}) = \sum_{n=0}^{N-1} \mathrm{e}^{i\,\mathrm{Q}na} \qquad |S_N(\mathrm{Q})| = \frac{\sin(N\mathrm{Q}a/2)}{\sin(\mathrm{Q}a/2)}$$

$$\mathrm{Q} = (h + \xi)\mathrm{a}^* \qquad |S_N(\xi)| = \frac{\sin(N\pi\xi)}{\sin(\pi\xi)} \to N \text{ as } \xi \to 0$$

$$|S_N(\xi = \frac{1}{2N})| \approx \frac{1}{\pi/(2N)} = \left(\frac{2}{\pi}\right) N \approx \frac{N}{2}$$

Kinematická teorie

$$F^{\text{crystal}} = \sum_{\text{n}} f(\mathbf{Q})\, \text{e}^{i\,\mathbf{Q}\cdot\mathbf{R}_{\text{n}}}$$

$$I = \left\langle \sum_{\text{m}} f(\mathbf{Q})\, \text{e}^{i\,\mathbf{Q}\cdot(\mathbf{R}_{\text{m}}+\mathbf{u}_{\text{m}})} \sum_{\text{n}} f^{*}(\mathbf{Q})\, \text{e}^{-i\,\mathbf{Q}\cdot(\mathbf{R}_{\text{n}}+\mathbf{u}_{\text{n}})} \right\rangle$$

$$= \sum_{\text{m}} \sum_{\text{n}} f(\mathbf{Q}) f^{*}(\mathbf{Q})\, \text{e}^{i\,\mathbf{Q}\cdot(\mathbf{R}_{\text{m}}-\mathbf{R}_{\text{n}})} \left\langle \text{e}^{i\,\mathbf{Q}\cdot(\mathbf{u}_{\text{m}}-\mathbf{u}_{\text{n}})} \right\rangle$$

$$\left\langle \text{e}^{i\,\mathbf{Q}\cdot(\mathbf{u}_{\text{m}}-\mathbf{u}_{\text{n}})} \right\rangle = \left\langle \text{e}^{i\,Q(u_{Q\text{m}}-u_{Q\text{n}})} \right\rangle$$

$$\left\langle \text{e}^{i\,x} \right\rangle = \text{e}^{-\frac{1}{2}\langle x^2 \rangle}$$

$$\left\langle \text{e}^{i\,Q(u_{Q\text{m}}-u_{Q\text{n}})} \right\rangle = \text{e}^{-\frac{1}{2}\langle Q^2 (u_{Q\text{m}}-u_{Q\text{n}})^2 \rangle}$$

$$= \text{e}^{-\frac{1}{2} Q^2 \langle (u_{Q\text{m}}-u_{Q\text{n}})^2 \rangle}$$

$$= \text{e}^{-\frac{1}{2} Q^2 \langle u_{Q\text{m}}^2 \rangle} \text{e}^{-\frac{1}{2} Q^2 \langle u_{Q\text{n}}^2 \rangle} \text{e}^{Q^2 \langle u_{Q\text{m}} u_{Q\text{n}} \rangle}$$

Kinematická teorie

$$e^{Q^2\langle u_{Qm}u_{Qn}\rangle} = 1 + \left\{e^{Q^2\langle u_{Qm}u_{Qn}\rangle} - 1\right\}$$

$$e^{-Q^2\langle u_Q^2\rangle/2} \text{ as } e^{-M}$$

$$I = \sum_m \sum_n f(\mathbf{Q})\, e^{-M} e^{i\,\mathbf{Q}\cdot\mathbf{R}_m}\; f^*(\mathbf{Q})\, e^{-M} e^{-i\,\mathbf{Q}\cdot\mathbf{R}_n}$$
$$+ \sum_m \sum_n f(\mathbf{Q})\, e^{-M} e^{i\,\mathbf{Q}\cdot\mathbf{R}_m}\; f^*(\mathbf{Q})\, e^{-M} e^{-i\,\mathbf{Q}\cdot\mathbf{R}_n} \left\{e^{Q^2\langle u_{Qm}u_{Qn}\rangle} - 1\right\}$$

$$f^{\text{atom}} = f(\mathbf{Q})\, e^{-\frac{1}{2}Q^2\langle u_Q^2\rangle} \equiv f(\mathbf{Q})\, e^{-M}$$

Kinematická teorie

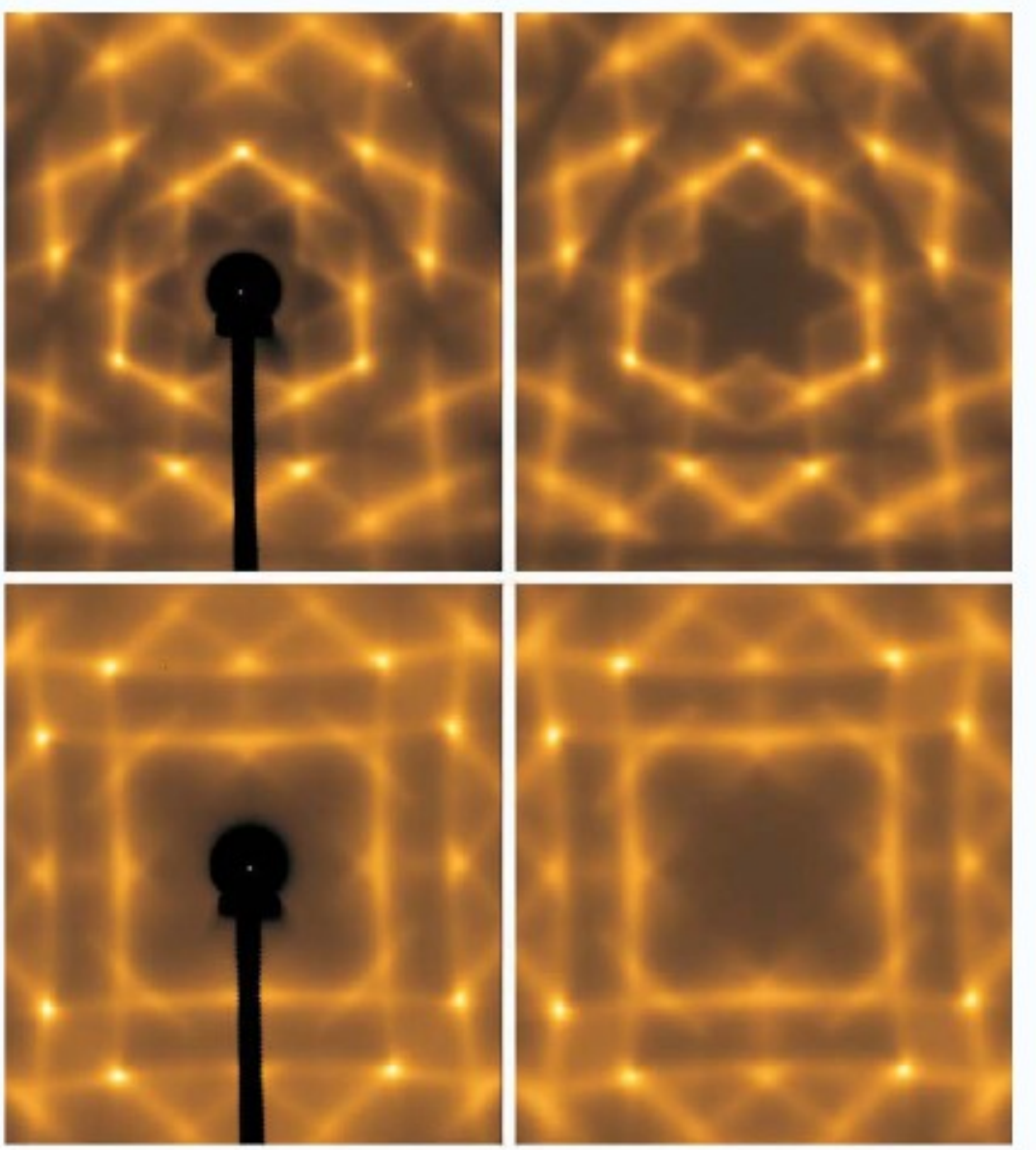

Fig. 5.14 Thermal diffuse scattering (TDS) from Si. The data were collected in a transmission geometry (photon energy 28 keV) using an image plate detector. The data were collected on the UNI-CAT beamline at the Advanced Photon Source in an exposure time of ~10 s. The top and bottom left panels show the data taken with a (111) and a (100) axis parallel to the incident beam respectively. The data are plotted on a logarithmic scale. The brighter spots are not Bragg peaks, as the Laue condition is never exactly fulfilled, but are due to the build up of TDS close to the position of where the Bragg peaks would occur. The right panels show the corresponding calculated images based on a simultaneous pixel-by-pixel fit to the data [Holt et al., 1999].

Kinematická teorie

$$\int \rho_e(r)\exp(-iQr)dr$$

$$F = \sum_{n=1}^{N} f_n \exp\left(iQ\mathbf{r}_n\right)$$

$$f_T = f\exp\left(-8\pi\overline{u^2}\sin^2\theta/\lambda^2\right)$$

$$F_{hkl}(T) = \sum_{n=1}^{N} f_n \exp\left(-B_n(T)\sin^2\theta/\lambda^2\right)\exp\left(2\pi i(hx_n + ky_n + lz_n)\right)$$

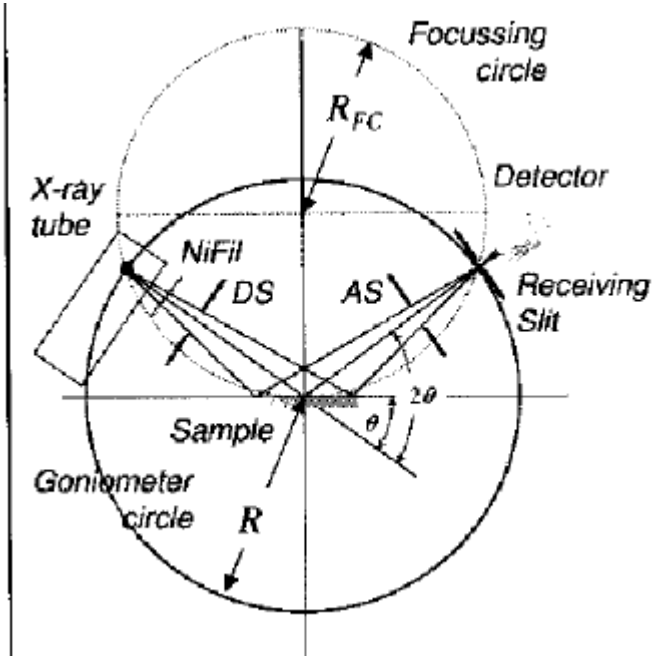

Multiplicity

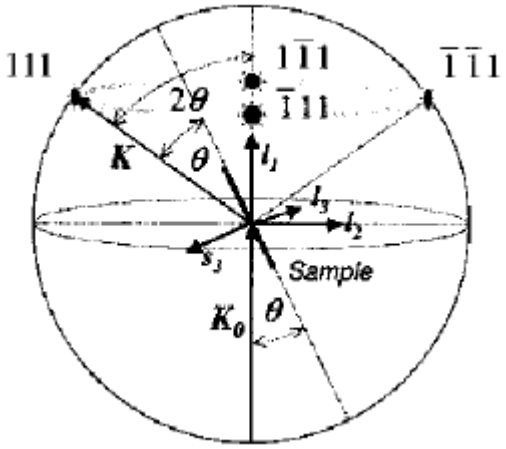

Geometry Factor

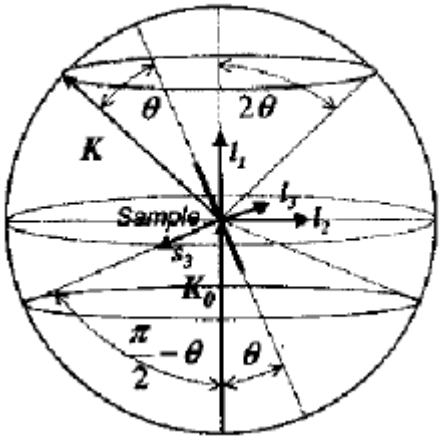

Length of Debye ring

$1/\sin 2\theta.$

$\cos\theta.$ Density of Q vectors

$G = \cos\theta/\sin 2\theta = 1/(2\sin\theta)$

Kinematická teorie

Polarization Factor

$$\overline{C^2} = \frac{1+\cos^2 2\theta}{2}$$

Absorption Factor

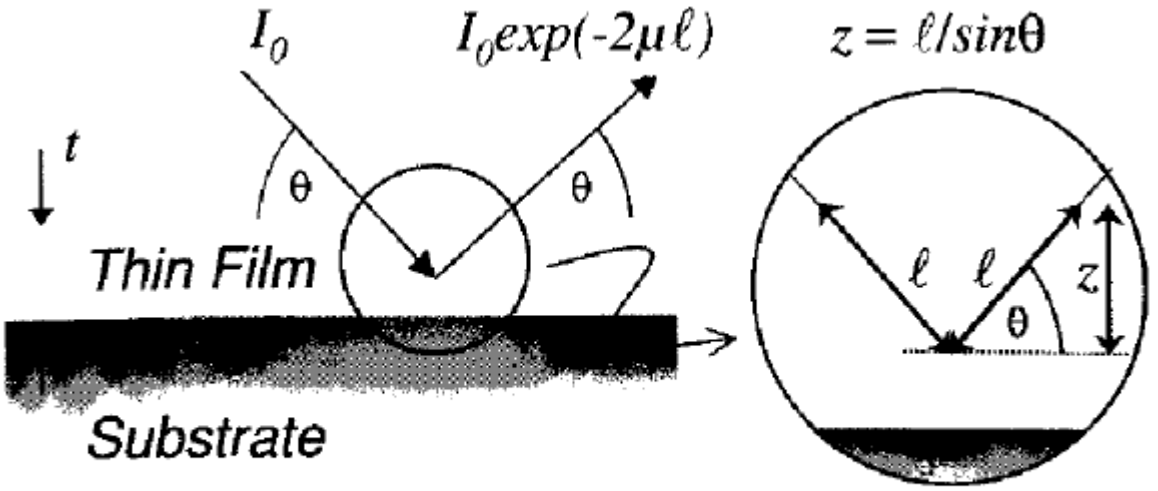

Figure 1.15 Schematic representation of the absorption effect for a thin-film sample in a $\theta/2\theta$ scan.

$$\int_0^{\ell_{max}} \exp(-2\mu\ell)d\ell \qquad \frac{1}{2\mu}\left\{1-\exp\left(-\frac{2\mu t}{\sin\theta}\right)\right\}$$

$$A = \int_0^t \Big/ \int_0^\infty \qquad A_{\theta 2\theta} = \left(1-\exp\left(-\frac{2\mu t}{\sin\theta}\right)\right)$$

Konečný proti nekonečnému vzorku

Kinematická teorie

Integration of the Interference Function

$$I(\boldsymbol{R})dSdt' = I_0 \frac{r_e^2}{R^2}\left|F_h\right|^2 m_h T_h G\overline{C^2} \frac{A_{\theta 2\theta}(t)}{2\mu} \prod_{i=1}^{3} \frac{\sin^2\left(N_1 a\boldsymbol{Q}\boldsymbol{c}_i / 2\right)}{\left(a\boldsymbol{Q}\boldsymbol{c}_i / 2\right)^2} dSdt'$$

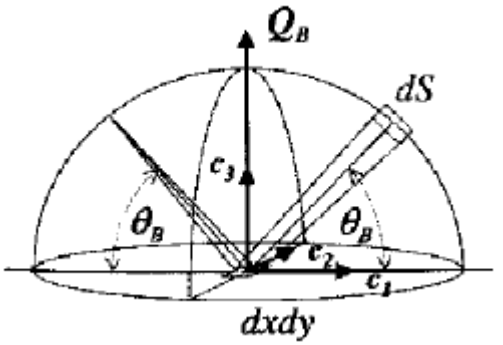

$$dS = R^2 \sin\theta dxdy$$

$$dxdy = \left(\frac{\lambda}{4\pi\sin\theta}\right)^2 d(\boldsymbol{Q}\boldsymbol{c}_1)d(\boldsymbol{Q}\boldsymbol{c}_2)$$

$$dS = \frac{R^2\lambda^2}{4a^2 4\pi^2 \sin\theta} d(a\boldsymbol{Q}\boldsymbol{c}_1)d(a\boldsymbol{Q}\boldsymbol{c}_2)$$

$$I(\boldsymbol{R})dSd(\Delta\theta) = I_0 \frac{r_e^2}{R^2\dot{\theta}}\left|F_h\right|^2 m_h T_h G\overline{C^2} \frac{A_{\theta 2\theta}(t)}{2\mu} \prod_{i=1}^{3} \frac{\sin^2\left(N_i a\boldsymbol{Q}\boldsymbol{c}_i / 2\right)}{\left(a\boldsymbol{Q}\boldsymbol{c}_i / 2\right)^2} dSd(\Delta t$$

$$\iiint \prod_{i=1}^{3} \frac{\sin^2\left(N_i a\boldsymbol{Q}\boldsymbol{c}_i / 2\right)}{\left(a\boldsymbol{Q}\boldsymbol{c}_i / 2\right)^2} d\left(a\boldsymbol{Q}\boldsymbol{c}_i / 2\right) = N_1 N_2 N_3$$

$$N_1 N_2 N_3 = \frac{V}{a^3} = \frac{V}{V_{uc}}$$

$$I_h = I_0 \frac{r_e^2}{\dot{\theta}} \lambda^3 m_h T_h \frac{1+\cos^2\theta}{\sin\theta\sin 2\theta} \frac{\left|F_h\right|^2}{V_{uc}^2} V \frac{A_{\theta 2\theta}(t)}{2\mu}$$

Kinematická teorie

Accurate Determination of Lattice Parameter

$$a = \frac{\lambda\sqrt{h^2+k^2+l^2}}{2\sin\theta_B}$$

$$\sin\left(\theta_0 - \frac{1}{2}\sum\Delta(2\theta)_i\right) = \frac{\lambda\sqrt{h^2+k^2+l^2}}{2a}$$

1. *Zero shift.* $\Delta(2\theta)_1 = c$

2. *Height misalignment.* $\Delta(2\theta)_2 = -2b\cos\theta / R$

3. *Sample transparency.*

$$\Delta(2\theta)_3 = -\frac{2}{R}\langle z\rangle\cos\theta$$

$$\langle z\rangle = \frac{\int_0^t z\exp(-2\mu t/\sin\theta)dz}{\int_0^t \exp(-2\mu t/\sin\theta)dz} = \frac{\sin\theta}{2\mu}\left\{1 + \frac{2\mu t/\sin\theta}{1-\exp(2\mu t/\sin\theta)}\right\}$$

$$\Delta(2\theta)_3 = -t\cos\theta / R$$ Thin sample

4. *Flat sample.* $\Delta(2\theta)_4 = -\frac{\delta_{ds}^2}{6}\cot\theta$ Divergence slit openin

5. *Axial divergence.*

$$\Delta(2\theta)_{5,\text{oneSol}} = -\frac{1}{12}\left(\delta_{\text{Sol}}^2 + \frac{B_a^2}{R^2}\right)\cot 2\theta$$

1 Soller, B délka ohniska

$$\Delta(2\theta)_{5,\text{twoSol}} = -\frac{\delta_{\text{Sol}}^2}{6}\cot 2\theta$$

2 Soller

Kinematická teorie

Line profile analysis

$$f_C(2\theta) = \left[1 + (2\theta - 2\theta_0)^2 / w^2\right]^{-1}$$
$$f_G(2\theta) = \exp\left[-\ln 2(2\theta - 2\theta_0)^2 / w^2\right]$$

$$\beta = \frac{1}{I_0}\int_{-\infty}^{\infty} I(2\theta)d2\theta$$ Integrální šířka

$$f_P(2\theta) = \left[1 + (\sqrt[m]{2} - 1)(2\theta - 2\theta_0)^2 / w^2\right]^{-m}$$ Pearsonova funkce

$$f_V(2\theta) = \frac{\beta}{\beta_C \beta_G}\int_{-\infty}^{+\infty} f_C(\xi) f_G(2\theta - \xi)d\xi$$ Voigtova funkce

$$\beta = \frac{\beta_G \exp(-k^2)}{1 - \mathrm{erfc}(k)} \qquad k = \frac{\beta_C}{\sqrt{\pi}\beta_G}$$

$$f_{pV}(2\theta) = \eta f_C(2\theta) + (1 - \eta) f_G(2\theta)$$ Pseudo-Voigt

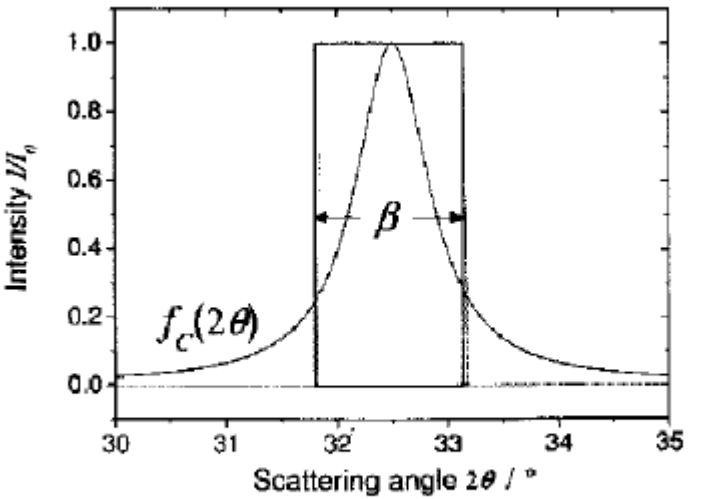

Figure 3.2 Visualization of the concept of integral breadth.

Table 3.1 Integral breadths of the five most relevant model functions in LPA, where $\Gamma(x)$ is the gamma function, $A = 0.9039645$, $B = 0.7699548$, $C = 1.364216$, $D = 1.136195$ and $E = 2(\ln 2/\pi)^{1/2} = 0.9394372$.

Model function	Equation	Integral width β
Cauchy	(3.2)	πw
Gauss	(3.2)	$\sqrt{\pi / \ln 2}\, w$
Pearson	(3.5)	$\frac{\pi 2^{2(1-m)}\Gamma(2m-1)}{(2^{1/m}-1)\left[\Gamma(m)\right]^2} w$
Voigt	(3.6)	$\frac{2(1 + Ck + Dk^2)}{E(1 + Ak + Bk^2)} w$
Pseudo-Voigt	(3.9)	$\left(\eta\pi + (1-\eta)\sqrt{\pi \ln 2}\right) w$

Kinematická teorie

Instrumental Line Profile

$$h(2\theta) = f(2\theta) \otimes g(2\theta) = \int_{-\infty}^{\infty} f(2\theta) g(2\theta - \xi) d\xi$$

$$\theta_2 = \arcsin\left(\frac{\lambda_{\alpha 2}}{\lambda_{\alpha 1}} \sin\theta_1\right)$$

$$I_1(2\theta) = I_{1+2}(2\theta) - R_{21} I_{1+2}\left(2\theta - 2\arcsin\left(\frac{\lambda_{\alpha 2}}{\lambda_{\alpha 1}} \sin\theta\right)\right)$$

$$\beta^2_{\text{instr}} = A\tan^2\theta + B + C\cot^2\theta + D\sin^2 2\theta$$

$\beta_h = \beta_f + \beta_g$ (pure C)

$\beta_h = \sqrt{\beta_f^2 + \beta_g^2}$ (pure G)

$$\beta_C^f = \beta_C^h - \beta_C^g$$
$$\left(\beta_G^f\right)^2 = \left(\beta_G^h\right)^2 - \left(\beta_G^g\right)^2$$

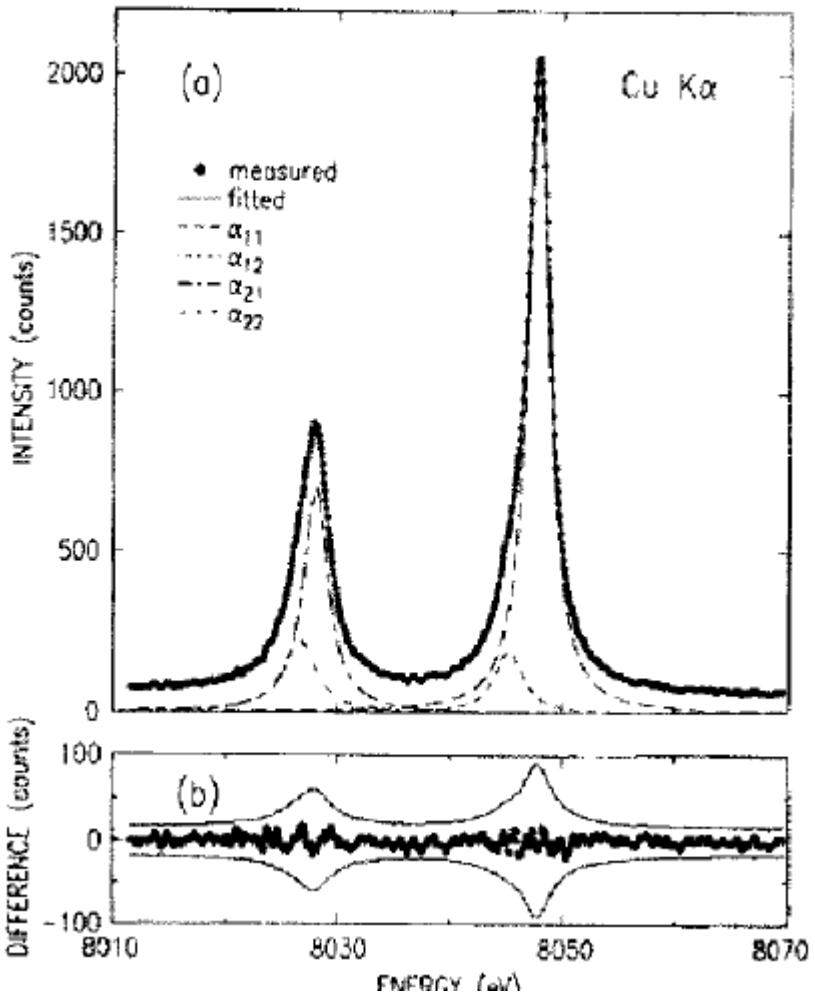

Table 3.2 Line parameters of the phenomenological decomposition of Cu Kα into four Lorentz/Cauchy functions [15].

Component	$\alpha_{1,1}$	$\alpha_{1,2}$	$\alpha_{2,1}$	$\alpha_{2,2}$
Energy (eV)	8047.837(2)	8045.367(22)	8027.993(5)	8026.504(14)
Intensity I_0	0.957(2)	0.090(1)	0.334(1)	0.111(1)
Width (eV)	2.285(3)	3.358(27)	2.666(7)	3.571(23)

Kinematická teorie

Reflection Broadening by Small Crystallite Size Only

$$\Im_{\mathrm{cub}}(Q) = \frac{\sin^2\left(aN_3Q/2\right)}{\sin^2\left(aQ/2\right)}$$

$$\int_{-1/2}^{1/2} \frac{\sin^2 \pi N_3 \xi}{\sin^2 \pi \xi} d\xi = N_3$$

$$\beta_Q = \frac{I_{\mathrm{int}}}{I_0} = \frac{2\pi N_3}{a}\frac{1}{N_3^2} = \frac{2\pi}{D_{\mathrm{cub}}}$$

$$D_{\mathrm{cub,mono}} = \frac{\lambda}{\beta_{2\theta}\cos\theta_0}$$

FWHM $\quad 2\sqrt{(\ln 2)/\pi} = 0.9394$

$$\Im_{\mathrm{sph}}(Q) = \frac{\sin^2 QR + QR(QR - \sin 2QR)}{Q^2R^2\sin^2\left(aQ/2\right)}$$

$$D_{\mathrm{sph}} = \sqrt[3]{\frac{6}{\pi}} D_{\mathrm{cub}} = 1.2407 D_{\mathrm{cub}} \qquad D_{\mathrm{sph,mono}} = \frac{4}{3}\sqrt[3]{\frac{\pi}{6}}\frac{\lambda}{\beta_{2\theta}\cos\theta_0}$$

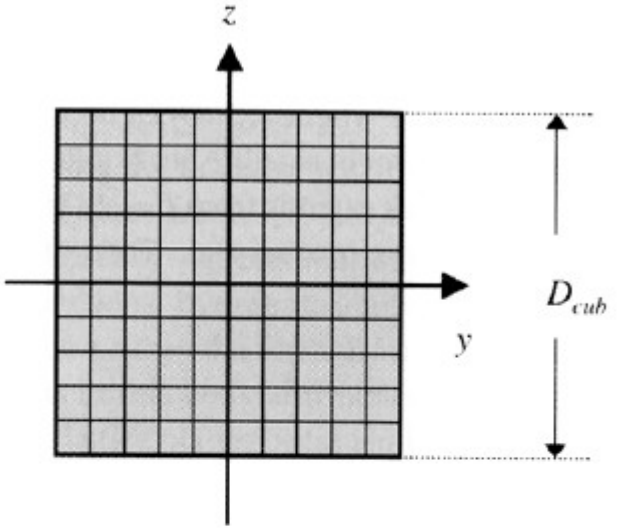

(a)

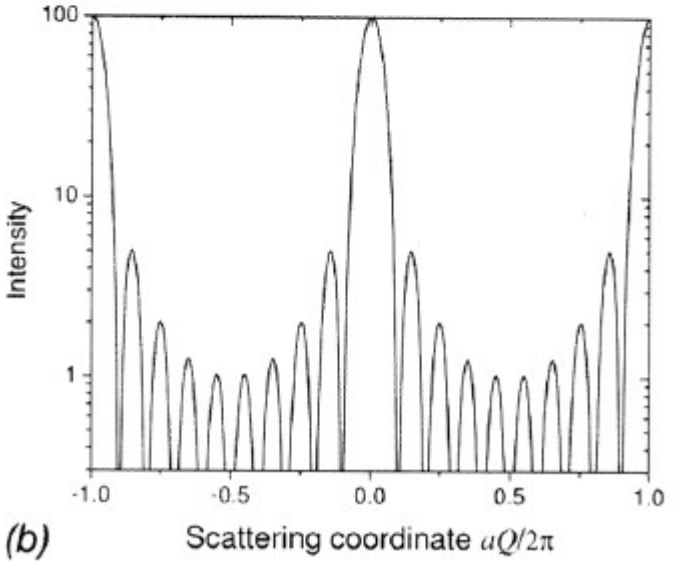

(b)

Kinematická teorie

$$D_{\text{mono}} = \frac{K_S \lambda}{\beta_{2\theta} \cos\theta_0}$$

Table 3.3 Scherrer constants K_S for some crystallite shapes. The conventions are obeyed that $h = |h|$, $k = |k|$, $l = |l|$, $h \geq k \geq l$, $S_1 = h + k + l$ and $S_2 = h^2 + k^2 + l^2$ (from Ref. [28]).

Shape	$h \geq k + l$	$h \leq k + l$
Sphere	$(4/3)(\pi/6)^{1/3}$	
Cube	$6h^3 / S_2^{1/2}(6h^2 - 2(k+l)h + kl)$	
Tetrahedron	$2h / 3^{1/3} S_2^{1/2}$	$S_1 / 3^{1/3} S_2^{1/2}$
Octahedron	$\frac{2S_1^3}{6^{1/3} S_2^{1/2}(S_1^2 + (k+l)S_1 + 2kl)}$	$\frac{2S_1^3}{6^{1/3} S_2^{1/2}(2S_1^2 - S_2)}$

It has been shown [27] by Stokes and Wilson already in 1942 that the size parameter derived from the Scherrer equation accounts for the ratio of the fourth central moment over the third moment of the crystallite size distribution function $g(D)$

$$\langle D \rangle_V = \langle D^4 \rangle / \langle D^3 \rangle$$

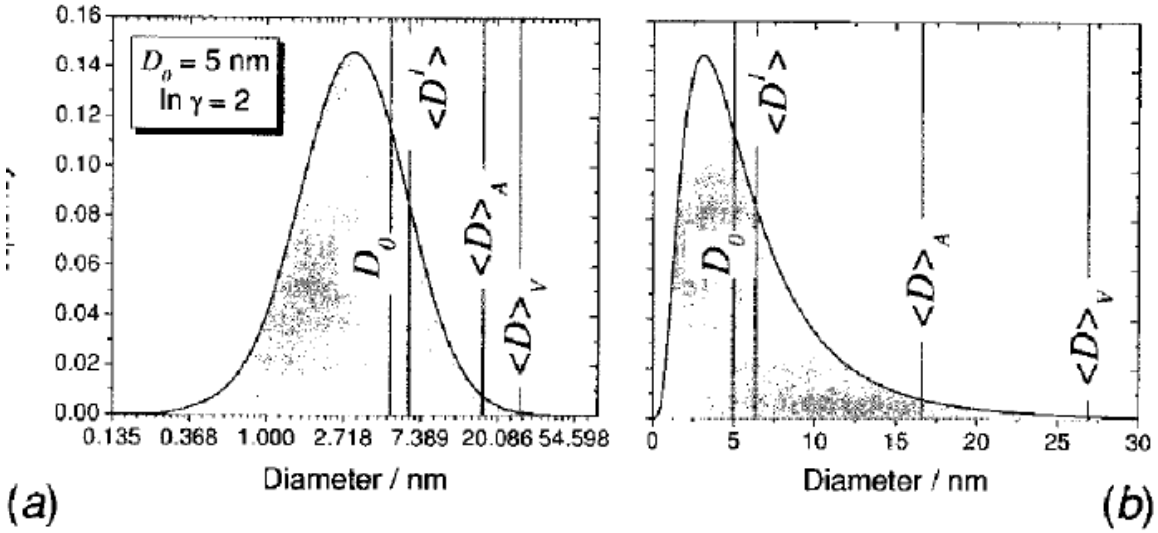

Figure 3.11 Logarithmic normal function with (a) a $\ln(D/D_0)$ abscissa and (b) a linear abscissa. The shape in (a) is of the same form as the Gauss bell function on a linear scale. The different averages of the lognormal distribution are indicated.

Kinematická teorie

Concomitant Occurrence of Size and Strain Broadening

$$\frac{\Delta d}{\Delta(2\theta)} = \frac{\lambda\cos\theta}{4\sin^2\theta} = \frac{d_0}{2}\cot\theta \qquad \beta_D = 2K_D\varepsilon_{rms}\tan\theta \qquad \varepsilon_{rms} = \langle\varepsilon^2\rangle^{1/2}$$

Analysis According to Williamson and Hall

$$\beta = \beta_S + \beta_D \qquad \beta_{2\theta} = \frac{K_S\lambda}{\langle D\rangle_V\cos\theta} + 2K_D\varepsilon_{rms}\tan\theta$$

$$\beta_{2\theta}\frac{\cos\theta}{\lambda} = \frac{K_S}{\langle D\rangle_V} + K_D\varepsilon_{rms}\frac{2\sin\theta}{\lambda}$$

$$\bar{C}_{hkl} = \bar{C}_{h00}(1 - q\Gamma^2_{hkl}) \qquad \Gamma_{hkl} = \frac{h^2k^2 + h^2l^2 + k^2l^2}{(h^2+k^2+l^2)^2} \qquad \beta_{2\theta}\frac{\cos\theta}{\lambda} = \frac{K_S}{\langle D\rangle_V} + \varepsilon\sqrt{\bar{C}_{hkl}}\frac{2\sin\theta}{\lambda}$$

Table 3.4 Dislocation contrast factors for (110) slip planes in bcc-structured α-Fe [39].

Reflection	$\bar{C}^{edge}_{hkl}$	$\bar{C}^{screw}_{hkl}$
110, 220, 211	0.1781	0.1040
200	0.2648	0.3055
310	0.2335	0.2330
222	0.1492	0.03684

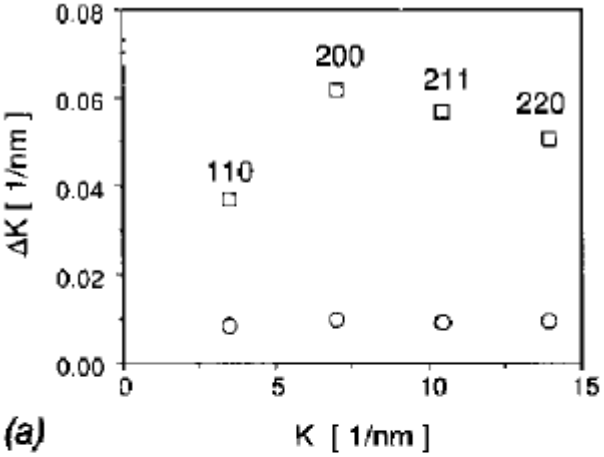

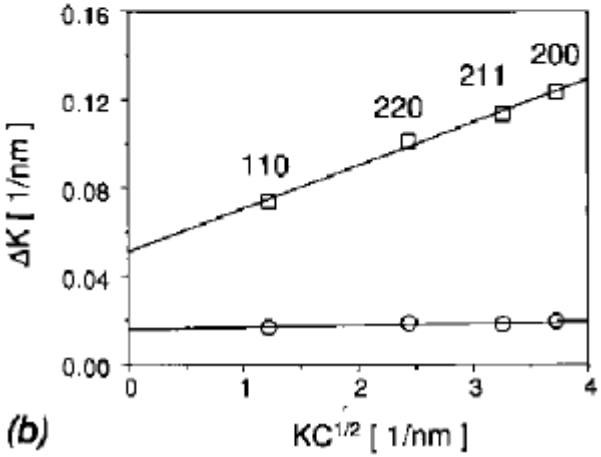

Method of Warren and Averbach

$$\Im(Q) = \frac{1}{N}\sum_{L} A(L)\cos(QL) \qquad A^{D}(L) = \exp(-2\pi^2 L^2 h^2 \langle \varepsilon_L^2 \rangle / a^2)$$

$$A(L) = A^{S}(L)A^{D}(L) \qquad \ln A(L) \approx \ln A^{S}(L) - 2\pi^2 L^2 h^2 \langle \varepsilon_L^2 \rangle / a^2$$

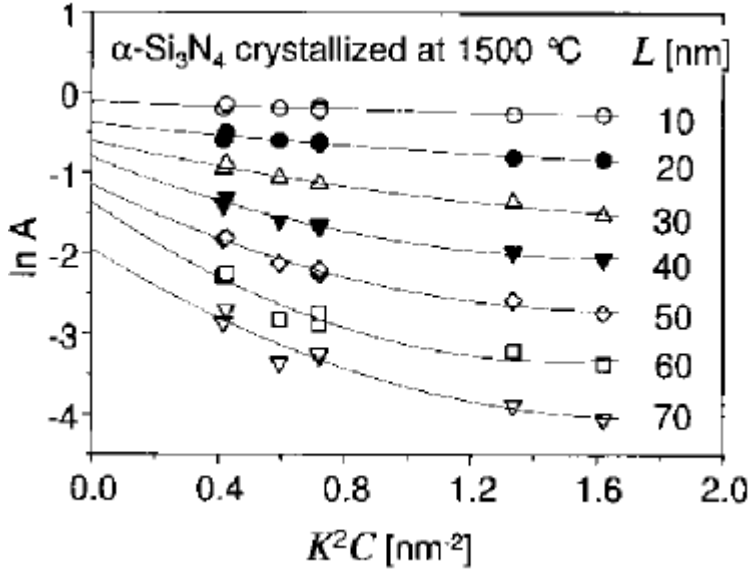

Single-Line Analysis

$$h_C = f_C \otimes g_C$$
$$h_G = f_G \otimes g_G$$

$$\langle D \rangle_v = K_S \lambda / (\beta_C^f \cos\theta)$$
$$\tilde{\varepsilon} = \frac{1}{4}\beta_G^f \cot\theta$$

Deconvolution by Fourier Techniques

$$I(Q) = \frac{\lambda}{2\pi \cos\theta} I(2\theta)$$

$$\beta_Q = \beta_{2\theta} \frac{dQ}{d(2\theta)} = \beta_{2\theta} \frac{2\pi \cos\theta}{\lambda}$$

$$H_n = \sum_{j=0}^{N-1} h(Q_j) \cos(2\pi nj / N)$$

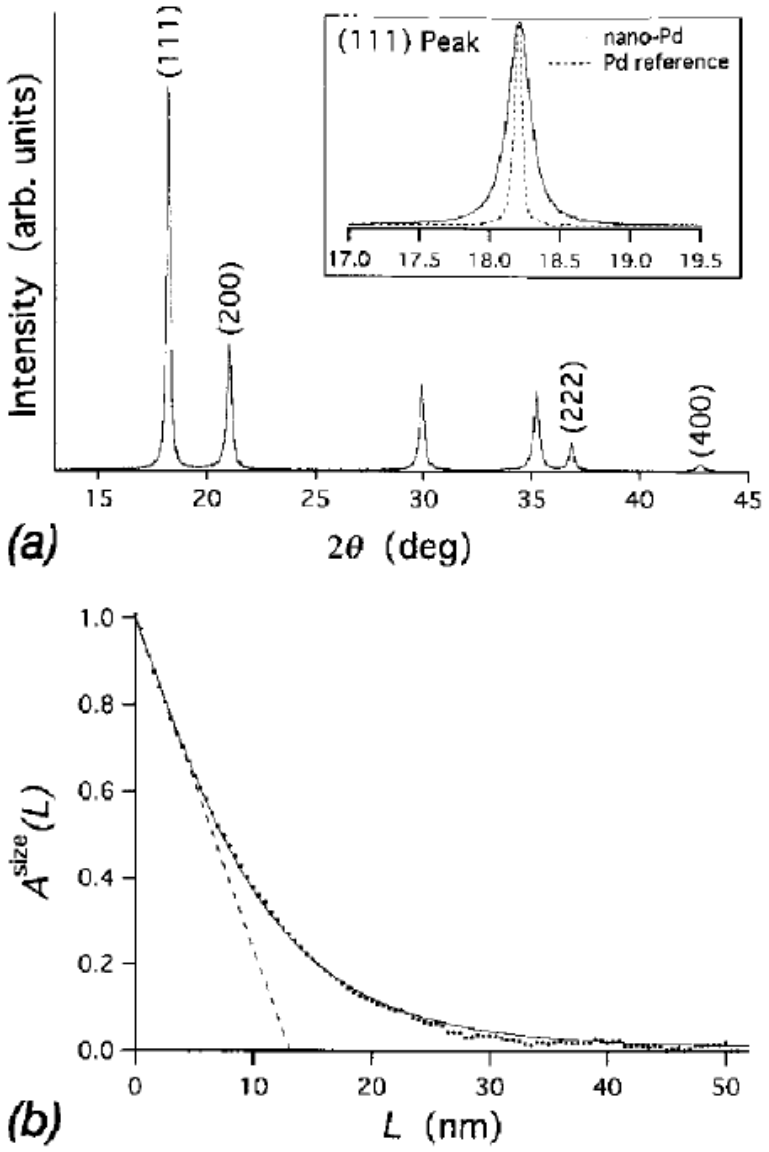

Figure 3.6 (a) $\theta/2\theta$ diffraction pattern of a nanocrystalline Pd powder sample measured with Mo Kα radiation. (b) Fourier coefficients $A(L)$ of the 111 reflection as a function of the Fourier-conjugated coordinate L (from Ref. [22]).

$$y(2\theta) = B(2\theta) + \sum_i I_{0,i} f(2\theta - 2\theta_{0,i}, \beta_i, m_i, k_i, \eta_i, \ldots)$$

Rietveld

$$y(2\theta) = B(2\theta) + \sum_h I_{0,h} \exp(-\pi^2 (2\theta - 2\theta_{0,h})^2 / \beta_h^2)$$

$$\left|F_h(r_n)\right|^2 \propto I_{\text{int},h} = I_{0,h}\beta_h$$

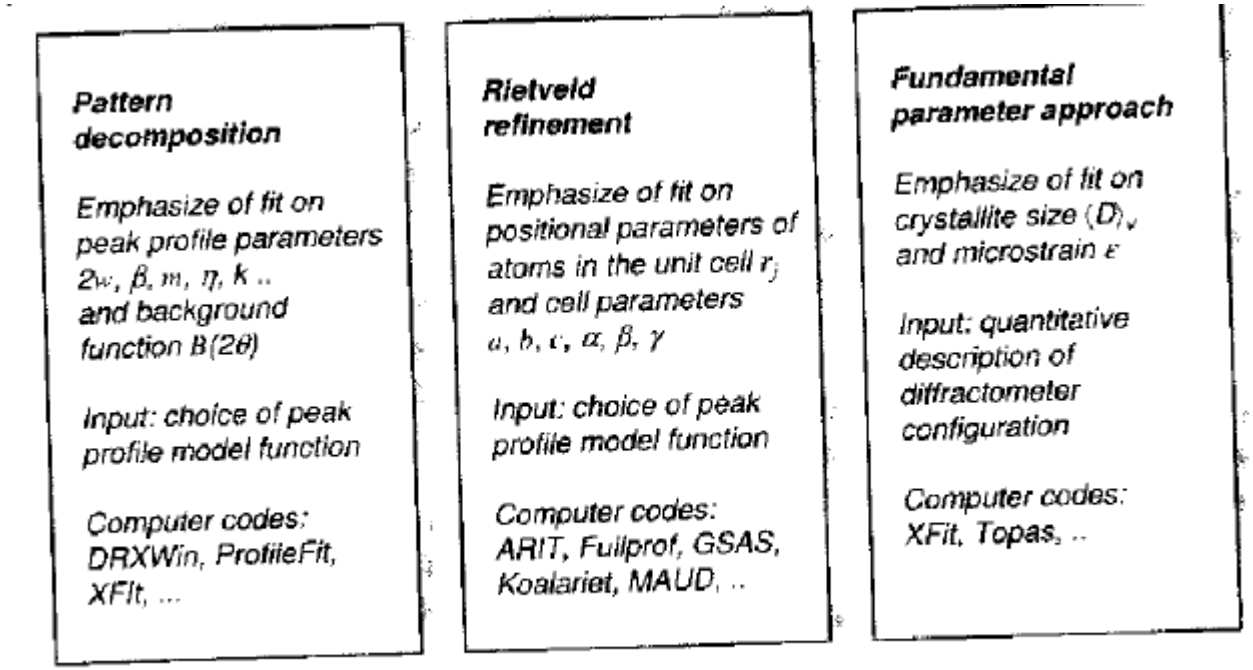

Figure 3.15 Different approaches in whole-pattern fitting.

Powder diffraction pattern as a function of various crystal structure, specimen, and instrumental parameters[5]

Pattern component	Crystal structure	Specimen property	Instrumental parameter
Peak position	Unit cell parameters (a, b, c, α, β, γ)	• Absorption • Porosity	• Radiation (wavelength), • Instrument/sample alignment • Axial divergence of the beam
Peak intensity	Atomic parameters (x, y, z, B, etc.)	• Preferred orientation • Absorption • Porosity	• Geometry and configuration • Radiation (Lorentz polarization)
Peak shape	• Crystallinity • Disorder • Defects	• Grain size • Strain • Stress	• Radiation (spectral purity) • Geometry • Beam Conditioning

$$H^2 = U \tan^2 \theta + V \tan \theta + W$$

Cagliotiho vztah pro šířku píku

$$I_{hkl} = K \times p_{hkl} \times L_\theta \times P_\theta \times A_\theta \times T_{hkl} \times E_{hkl} \times |F_{hkl}|^2$$

where:

- K: scale factor
- p_{hkl} : multiplicity factor, which accounts for symmetrically equivalent points in the reciprocal lattice
- L_θ: Lorentz multiplier, defined by diffraction geometry
- P_θ: polarization factor
- A_θ: absorption multiplier
- T_{hkl}: preferred orientation factor
- E_{hkl}: extinction factor (often neglected as it is usually insignificant in powders)
- F_{hkl}: structure factor as determined by the crystal structure of the material

For general application of the Rietveld method, irrespective of the software used, the observed Bragg peaks in a powder diffraction pattern are best described by the so-called peak shape function (PSF). The PSF is a convolution of three functions: the instrumental broadening $\Omega(\theta)$, wavelength dispersion $\Lambda(\theta)$, and the specimen function $\Psi(\theta)$, with the addition of a background function, $b(\theta)$. It is represented as follows:

$$PSF(\theta) = \Omega(\theta) \otimes \Lambda(\theta) \otimes \Psi(\theta) + b(\theta),$$

where $\otimes$ denotes convolution, which is defined for two functions f and g as an integral:

$$f(t) \otimes g(t) = \int_{-\infty}^{\infty} f(\tau)g(t-\tau)d\tau = \int_{-\infty}^{\infty} g(\tau)f(t-\tau)d\tau$$

$$I_i = P_i \,.\, Q_i \,.\, T_i \,.\, w_i \doteq P_i \,.\, Q_i \,.\, w_i ; \quad i = 1,2,.....,l \tag{1}$$

kde

Pi … přístrojový faktor (mění se od přístroje k přístroji podle detailů experimentálního uspořádání);

Qi … faktor daný ideální krystalovou strukturou dané fáze (polohami atomů v základní buňce krystalové struktury i-té fáze a jejich teplotními kmity kolem těchto poloh);

Ti …. faktor daný reálnou strukturou difraktujícího preparátu, tj. tím, jak velké jsou krystalky jednotlivých fází obsažených v preparátu, jaký je jejich tvar, orientace, umístění a nejrůznější odchylky od ideální krystalové struktury;

wi …. hmotnostní koncentrace i-té fáze v preparátu.

$$w_i = \frac{I_i}{P_i \, Q_i \, T_i} \doteq \frac{I_i}{P_i \, Q_i}$$

Kalibrace metodou vnějšího standardu

$$w_i = \frac{I_i}{I_o} \, \mu_m \, C_i$$

Kalibrace metodou vnitřního standardu

$$w_i = \frac{I_i}{I_o} \, w_o \, D_i$$